*Int. J. Electrochem. Sci.*, 10 **(2015)** 9933 - 9942

International Journal of
ELECTROCHEMICAL
SCIENCE
www.electrochemsci.org

# Study of Iridium electrodeposition on Ti and A304

*S.S. Serrano Lopez*[1], *V. E. Reyes Cruz*[1,*], *J. A. Cobos-Murcia*[1,2], *M. A. Veloz Rodríguez*[1], *J. Hernandez Avila*[1].

[1]Universidad Autónoma del Estado de Hidalgo, ÁreaAcadémica de Ciencias de la Tierra y Materiales,. Carretera Pachuca-Tulancingo Km. 4.5, C.P. 42184 Pachuca, Hidalgo, México.
[2] Consejo Nacional de Ciencia y Tecnología, Departamento de Cátedras. Av. Insurgentes Sur 1582, Col. Crédito Constructor, Delegación Benito Juárez, México D. F. C.P. 03840 México.
[*]E-mail: reyescruz16@yahoo.com

*Received:* 21 September 2015 / *Accepted:* 25 October 2015 / *Published:* 4 November 2015

Iridium is considered a valuable material due to its physical, chemical and electrocatalytic properties [1-3]. Iridium recovery from post-consumed industrial materials and effluents [4, 5] is necessary, since the natural resources for its production are limited and its demand in the industry will continue growing. This paper presents the electrochemical study of the iridium deposit on titanium (Ti) and stainless steel (A304) substrates in an electrolytic medium of HCl. Cyclic voltammetry results show iridium reduction response in standard solutions from 12.5 to 3 ppm for the two electrodes used. The study of the cathodic charge, current (i) vs. Potential (E) curves, the results of semi-quantitative chemical analysis by X-ray energy dispersive spectroscopy (EDS) and the diffusion coefficient of iridium $D_{Ir}$, confirm the deposit of iridium on Ti electrodes and A304.

**Keywords:** iridium, stainless steel, titanium, electrodeposition, iridium diffusion coefficient

## 1. INTRODUCTION

Iridium is considered a valuable material due to its physical, chemical and electrocatalytic properties [1-3]. The extraction of this metal in the world is limited, ranking 77th in abundance among the elements of the Earth crust [4, 5], that is the reason to encourage the Ir recovery from post-consumed industrial materials. Pyrometallurgical and hydrometallurgical techniques are used for the recovery of iridium; however, these techniques include the use of ionic resins, extraction with solvents and recovery by reducing agents. This requires large amounts of solvents and a limited recovery rate, given the low selectivity of the metal [6-8].

The electrochemical techniques represent an alternative in the recovery of the platinum group [9-13], yet iridium recovery through an electrochemical procedure has not been extensively explored [14-17]. The most recent research about electrochemical recovery of Ir, is that of the anodic deposit of iridium

oxidized particles on vitreous carbon [17], using a perchloric acid solution ($HClO_4$) with 1000 ppm of Ir species. So that, the research on the Ir deposit from sulphate and bromide solutions with Ir concentrations up to 2000 ppm [18]. Nevertheless, metallic massive deposition or recovering of iridium from post-consumed industrial materials is not considered. On the other hand, in a previous work of our group [4, 19], we used a less strong acid, i.e. hydrochloric acid to use in Iridium leaching. There, we have shown the feasibility of iridium electroleaching in the form of complexes in hydrochloric acid from post-consumed industry materials, obtaining a concentration of 3 ppm. In the Ir metallic recovering, chloride ion used to leach looks for the potential displacement to more negative values and to diminish the hydrogen evolution such as has been observed with deposit of other noble metals [20-22]. This paper presents the recovery of metallic iridium from standard solutions that simulate the concentration of iridium leach form post-consumed products in HCl medium, using electrochemical techniques, on stainless steel electrodes (A304) and Titanium (Ti). Energetic conditions found in this work will be used to carry out the Ir deposition from solutions with Ir low concentrations.

## 2. EXPERIMENTAL SECTION

### *2.1. Thermodynamic study*

Pourbaix diagrams of Ir- (acidic) were constructed using the computer program Hydra-Medusa from Royal Institute of Technology (KTH) Stockholm, Sweden in order to obtain thermodynamic conditions of E and pH for iridium electrochemical deposition. The system conditions were HCl 2M and $1.56x10^{-7}$ M of iridium, using $logK$= 0.35 and $logK$= 15.01 for complex species of Ir (IV) and (III).

### *2.2. Electrochemical study*

Voltammetric studies with cathodic direction were performed in a potential range between -0.3 and -1.0 V vs. SCE at a potential sweep rate of 25 $mV \bullet sec^{-1}$, for the two electrodes under study; with or without iridium. Chronoamperometric profiles were obtained in the potential range between -0.3 and -1.0 V vs. SCE during 600 seconds of electrolysis, with and without iridium, using Ti and A304 electrodes. After, i vs. E curves were constructed taking the data of the current of different potentials at an electrolysis time of 300 seconds. Chronopotentiometric profiles were obtained at a constant cathodic current of -47 mA during 7200 seconds for the two electrodes in study.

All experiments were performed in a conventional electrochemical cell of three electrodes. Titanium (Ti) and stainless steel (A304) were used as working electrodes, graphite as counter electrode and as reference standard calomel electrode (SCE). Electrolytic solutions were prepared with deionized water of high purity with 14.8 $m\Omega \bullet cm$ resistivity at three concentrations of iridium; 3, 6 and 12.5ppm. Solutions were prepared by dissolving a standard solution of 1000 ppm iridium in a 1 M solution of

hydrochloric acid, analytical grade and with a purity of 37%. The cell was coupled to the Princeton Applied Research potentiostat/galvanostat Model 263A equipment with a PowerSuite 2.56 interface.

### *2.3. Chemical characterization*

After the chronopotentiometric profile, the characterization of Ti and A304 electrodes was performed by scanning electron microscopy on a JEOL JSM-6300 microscope, operated at 30 KV power. The images were obtained by secondary electron emission. The semi-quantitative analysis on the studied electrodes was performed by Energy Dispersive Spectroscopy (EDS) of the emission signals K and L of the interest elements (Ir, C, Cl, Fe, Ti, W).

## 3. RESULTS AND DISCUSSION

### *3.1. Thermodynamic analysis*

Figure 1 shows the Pourbaix diagram with the thermodynamic conditions of the system Iridium (Ir) in hydrochloric acid (HCl). Figure 1 demonstrates that ionic species of $[IrCl_6]^{3-}$ is deposited in the pH range from 0 to 4.2 and lower potentials than 456 mV vs. SCE. The diagram also shows that the hydrogen evolution process does not interfere in the iridium deposit.

The reaction (1) of the iridium deposit is:

$[IrCl_6]^{3-} + 3e^- \rightarrow Ir + 6Cl^-$ E0 = 581 mV vs. SCE (1)

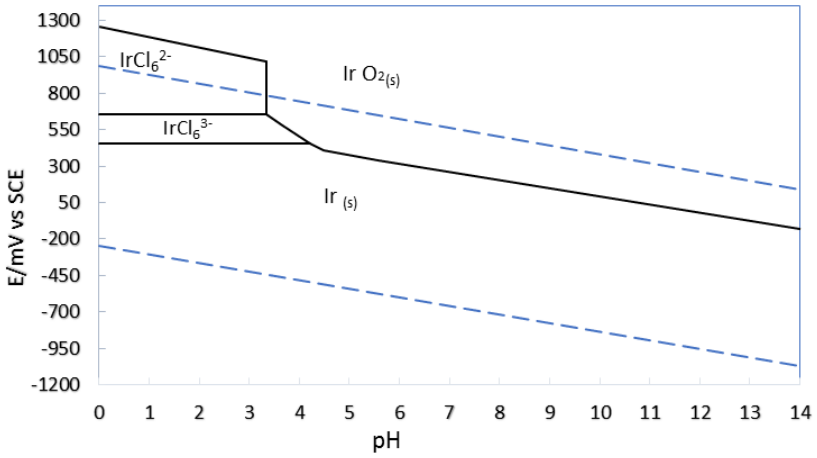


**Figure 1.** Pourbaix diagram of the system Ir-HCl with concentrations of iridium of $1.56x10^{-7}$ M and 2 M, respectively.

### *3.2. Kinetic analysis*

Figure 2 shows the voltammograms of Ti (2a) and A304 (2b) electrodes in 2 M HCl, without iridium (blue) and with 6 ppm (red). It can be observed on the figure (line blue) a reduction process,

C1, which starts from the potential -810 and -750 mV vs. SCE for Ti and A304, respectively; this process is attributed to hydrogen evolution. It is important to mention that the A304 electrode has a higher cathodic current compared to the Ti electrode for the potential -1000 mV vs. SCE (115 and 49 mA respectively). This behaviour is attributed to the substitution of the hydrogen adsorbed on the surface by the chloride ion, which is concordant with results of the literature [20, 22-24].

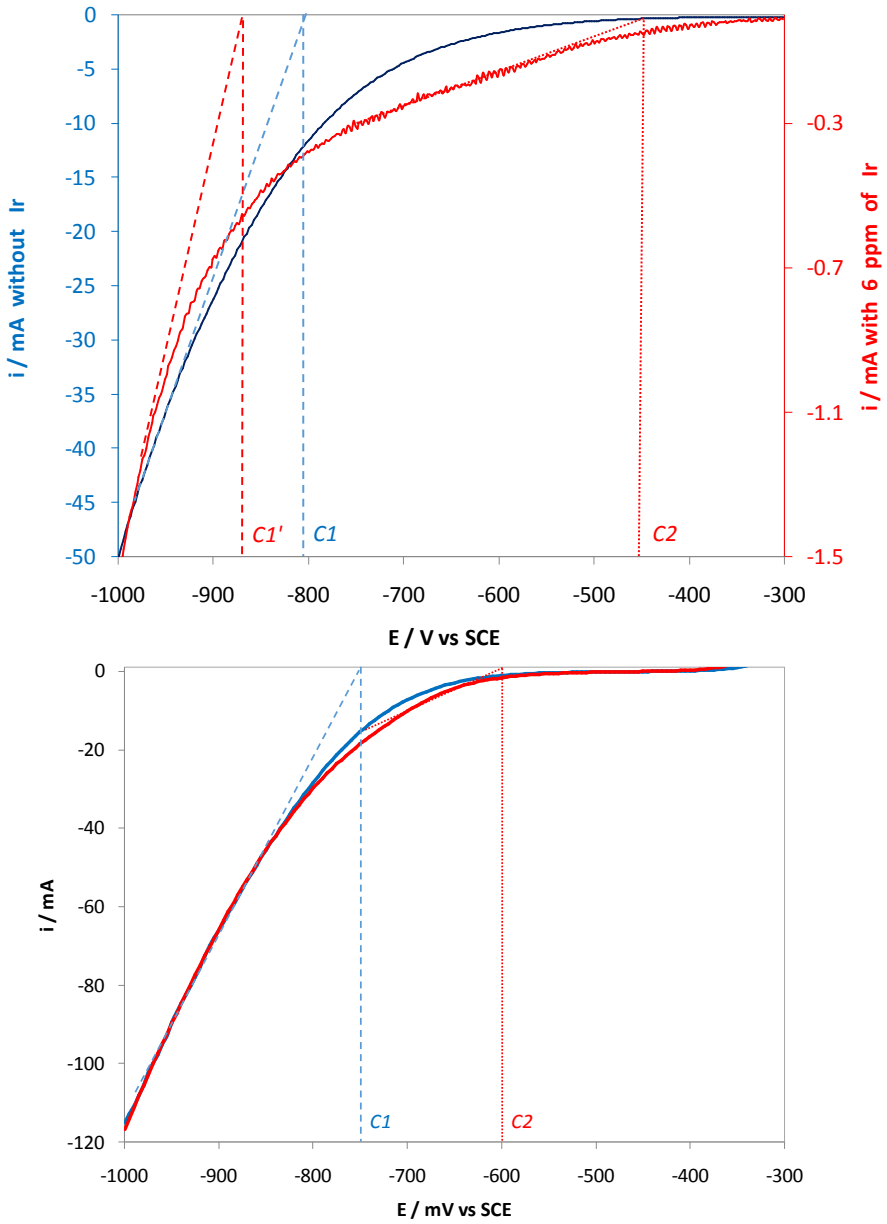


**Figure 2.** Voltammograms obtained from the electrodes (a) Ti and (b) A304 in a solution without iridium (blue) and [Ir]= 6 ppm at a sweep rate of 25 mV $s^{-1}$

The presence of iridium in the solution displaces the reduction potential of the process C1 within more cathodic values (-810 to -870 mV vs. SCE) for Ti, compared to the electrolyte without iridium (-610 mV vs. SCE). While the potential value for the process C1 on the A304 electrode remains without changes. In the figure 2 (red line), the current curve exhibits an increase, respect to the base line of the process C2, when iridium is present (for both electrodes) from the potential of -440 or -

600 mV vs. SCE for Ti and A304, respectively. This increase is attributed to Ir deposit on the different working electrodes under study. The deposition process is coupled to the hydrogen evolution and is carried out from -870 mV vs. SCE for the Ti electrode and -750 mV vs. SCE for the A304.

A study of cathodic charges was performed from the linear voltammograms with the aim of finding the effect that the Ir concentration has on the response of the reduction charge for the system (electrode/solution). Table 1 shows the cathodic charge calculated for both electrodes (Ti and A304) as a function of the Ir concentration (0, 3, 6 and 12.5 ppm).

Table 1 shows that, on Ti electrode, there is an important diminish on the cathodic charge when the Ir is present in the solution (plus to 97%) with the three concentrations under study, compared to the solution without Ir. This behaviour is associated to the adsorbed hydrogen substitution on the surface of the electrode by chloride and Iridium complex ($[IrCl_6]^{3-}$). This substitution modifies the kinetic and thermodynamic conduct; it depends on the electrode nature [18] and inhibit the electrochemical Ir deposition reaction as the hydrogen evolution. On the other hand, it is observed that when Ir concentration increases there is a slight increase in the cathodic charge, which is attributed mainly to the Ir deposition on Ti electrode.

In the case of the A304 electrode, there is an important increase of the cathodic charge of about 200% when Ir is present. This conduct is attributed to the lack of hydrogen substitution by the chloride ion, since soluble iron complex species with chloride are thermodynamically easier to obtain than the adsorbed chloride ones [18]. Iron complex species with chloride give place to increases on the Ir deposit and on the hydrogen evolution on A304 surface. Moreover, when the Ir concentration increases, the cathodic charge growths until it reaches a limit charge for the concentrations 6 and 12.5 ppm; which is indicative that the process is controlled by the electron transference.

**Table 1.** Cathodic charges obtained from the voltammograms and with different Ir concentrations in the electrolytic bath.

| | \|Ti \|\|Gr\| | \|A304\|\|Gr\| |
|---|---|---|
| [Iridium] / ppm | Charge / mC•cm-2 | |
| 0 | 67 | 310 |
| 3 | 2.5 | 672 |
| 6 | 4 | 842 |
| 12.5 | 5 | 840 |

It is worth to mention the use of the chloride ion has more adsorption on the Ti electrode surface and other noble metals [25] than the A304 electrode, where there is more cathodic charge.

In order to narrow the potential range and/or cathodic current where the iridium deposit is carried out, i vs. E curves were elaborated from chronoamperometric studies in the potential range of -300 to -1000 mV vs. SCE on Ti and A304 electrodes at 3 and 6 ppm which simulates the concentration of leached iridium from post-consumed materials of the ceramics industry.

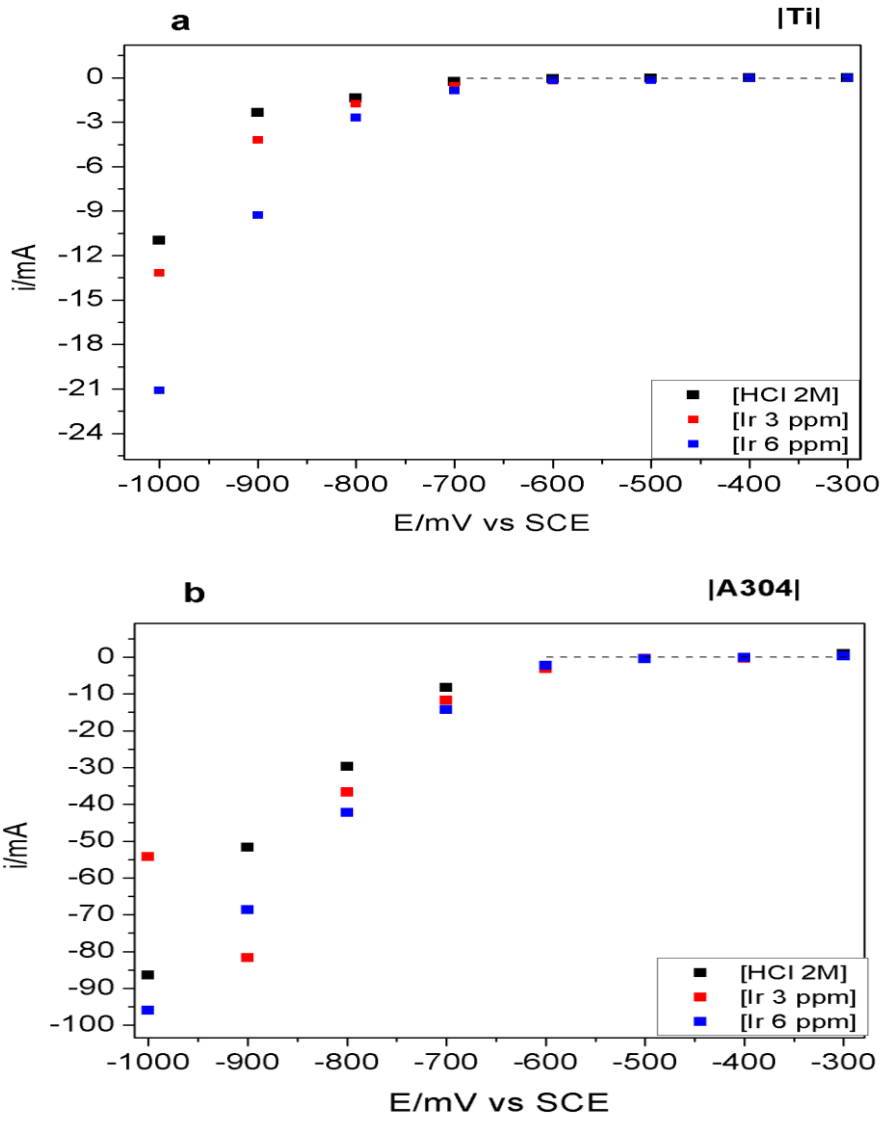


**Figure 4.** i vs. E curve obtained from the (a) Ti and (b) A304 electrodes chronoamperometric profiles at potential range -300 to -1000 mV vs. SCE.

Figure 4 shows that when the iridium concentration is increased, the cathodic current of iridium deposit rises in the Ti and A304 electrodes from a potential of -700 mV vs. SCE. Figure 4a demonstrates that the potential range for the Ir deposit with the least interference of the hydrogen evolution is -300 to -1000 mV vs. SCE for the Ti electrode at 3 and 6 ppm of iridium. While the current range for the Ir deposit on Ti for the concentration of 3 ppm is 0.5 a 13 mA and 1.1 a 21 mA for the concentration of 6 ppm.

Figure 4b shows that for the A304 electrode the potential range of Ir deposit with the least hydrogen evolution interference takes place from -300 to -800 mV vs. SCE for the 3 ppm iridium concentration. While the current range for the Ir deposit on A304 electrode for the 3 ppm concentration is 12 to 38 mA and 13 to 42 mA, for the 6 ppm concentration. It is important to mention that on A304 electrode the hydrogen evolution is observed from a potential of -800 mV vs. SCE.

The i vs. E curves indicate that the process of the Ir deposit is controlled by the mass transport in the potential range from -300 to -700 mV vs. SCE for Ti and -300 to -600 mV vs. SCE for A304 electrode. From the data obtained in the chronoamperometric studies the Ir diffusion coefficient ($D_{Ir}$) can be calculated by the Cottrell equation (Equation 1). This equation is restricted to deposition processes controlled by the mass transport of ionic complex on the electrode surface [12].

$$I(t) = \frac{nFAD^{1/2}C}{(\pi t)^{1/2}} \qquad \text{Equation (1)}$$

Where

$$D_{Ir} = \frac{m^2\pi}{(nFAC)^2}$$

In the equation *m* is the plotted slope from i vs. $t^{-1/2}$, *n* is the number of electrodes, *F* is the Faraday constant, *A* is the area of the working electrode, *C* is the concentration of the specie, t is time and D is the diffusion coefficient.

Table 2 shows the diffusion coefficient of Ir ($D_{Ir}$) calculated, pondering n=3, F= 96500 C/mol, C = 1.56x10-7 mol/$cm^3$ and the chronoamperometric profiles from the potentials -600 and -700 mV vs. SCE at 300 seconds for A304 and Ti electrodes respectively.

Table 2 demonstrates that the calculated value of $D_{Ir}$ is different for the two electrodes under study and has the same order of magnitude. The order of magnitude of the $D_{Ir}$ values of this research are consistent with those reported [26], $D_{Ir}$ de $4.95x10^{-1}cm^2s^{-1}$. The results of the $D_{Ir}$ values indicate that Ir can be deposited on the surfaces of the Ti and A304 electrodes.

**Table 2.** Diffusion coefficient of iridium ($D_{Ir}$) calculated on a 3 ppm solution of Ir ($1.56x10^{-7}$ molcm-$^3$).

| **Electrode** | **Area ($cm^2$)** | **chronoamperometric profiles** E/mV **vs. SCE** | **$D_{Ir}$ ($cm^2/s$)** | **R** |
|---|---|---|---|---|
| **Ti** | 0.50 | -700 | $1.25x10^{-1}$ | 0.8560 |
| **A304** | 0.20 | -600 | $6.47x10^{-1}$ | 0.9460 |

In order to verify the massive deposit on the studied substrates, chronopotentiometric analysis on a 3 ppm solution for 7200 seconds were performed with a constant current of -47 mA on both electrodes. Finally, the surfaces of the Ti and A304 electrodes were characterized semi-quantitatively using scanning electron microscopy and energy dispersive spectroscopy X-ray.

### *3.3. Chemical characterization*

Figure 5 shows images of scanning electron microscopy and energy emission spectrum of elements deposited upon the Ti electrode after performing a chronopotentiometric profile of -47 mA for 7200 seconds. Figure 5a of the electron microscopy image at 33X exhibits a low density of beads

on Ti compared to electrode A304. However, when a 300X amplification (Figure 5b) was obtained, a granular agglomerate size close to 200 microns is shown. In the emission spectrum (Figure 5c) the peaks of the Ir, Ti and Cl elements are observed. The Ti and Cl peaks are shown due to the base element electrode and the chlorine from the electrolyte.

Figure 6 shows the images of the scanning electron microscopy and the emission spectrum of the elements deposited on A304 after the chronopotentiometric profile at -47 mA during 7200 s.

Figure 6a of the electron microscopy at 16X presents the formation of deposits in beads form on the stainless steel (A304). Furthermore, it also shows that the deposits are irregular and that there is a greater amount in the lateral sides of the A304 electrode. The image at 100X (Figure 6b) shows the agglomerate of the deposit of 100 microns. The energy spectrum (Figure 6c) displays the emission peaks of the Ir, Fe and Cl elements.

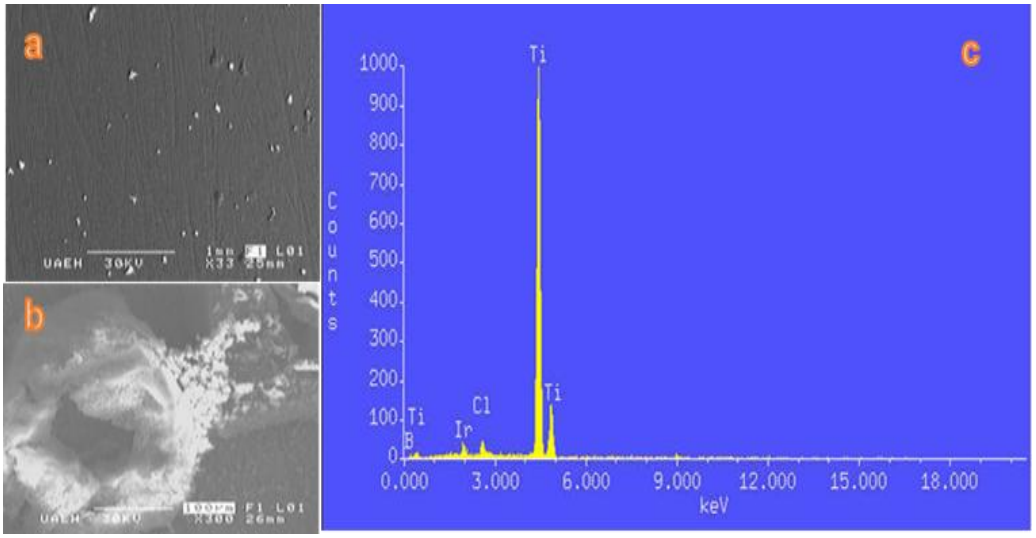


**Figure 5.** Microscopies at 33X (a) and 300x (b) and emission spectrum (c) of the Titanium electrode (Ti).

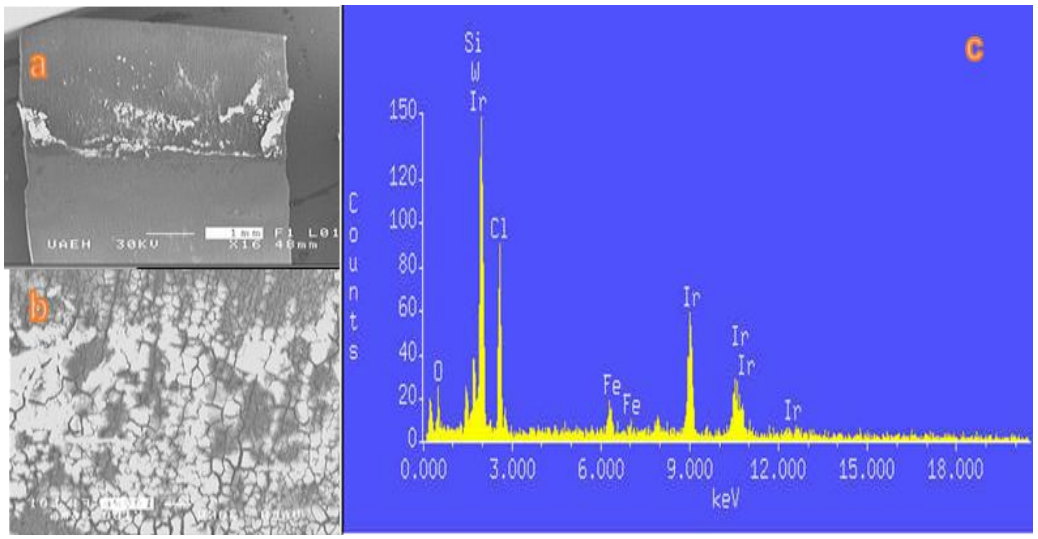


**Figure 6.** Microscopies at 16X (a) and 100 X (b) and emission spectrum (c) of the stainless steel electrode (A304).

The analysis by energy dispersive spectroscopy X-ray (EDS) indicates the iridium deposit of 5.09% (w/w) on A304 and 0.61% (w/w) on Ti. It is important to indicate that the potential of chronopotentiometric studies on A304 and Ti agrees with the potential of the Ir deposit determined by the curves i vs. E.

## 4. CONCLUSIONS

Thermodynamic studies indicate that the iridium deposit without interference of the hydrogen evolution is possible. While the electrochemical studies indicate that the Ir deposit on A304 and Ti surfaces, has the hydrogen evolution coupled on potentials above of -700 mV vs. SCE.

The potential displacement of reduction process at less negative values in the voltammograms and the changes in cathodic charge when iridium is present in the solution at different concentrations, indicate that the iridium deposit on the Ti and A304 electrodes surfaces is being carried out. i vs. E curves indicate that the massive deposit of iridium is reached from -700 mV vs. SCE for the electrode A304 and -800 mV vs. SCE for the Ti electrodes. Chemical analysis by EDS of the Ti and A304 electrodes after the chronopotentiometry, at a current of -47 mA for 7200 seconds, confirm the iridium deposit of 5.09 and 0.61% (w / w) on stainless steel (A304) and titanium (Ti) respectively. The $D_{Ir}$ is also confirming the Ir deposition. $D_{Ir}$ in this work is $6.47x10^{-1}$ $cm^2s^{-1}$.

A304 is the best electrode to carry out the Ir deposition from low concentration solutions which come from the leaching of post-consumed materials in chloride medium; due to the low adsorption of the chloride ion on the A304 surface.

ACKNOWLEDGMENTS
The authors thank UAEH for the infrastructure used and PROFOCIES federal program in the preparation of this article. JACM acknowledges support of Cátedras CONACYT program.

## References

1. D. R. Wilburn and D. I. Bleiwas, *Platinum-Group Metals.* U.S. Geological Survey (2004)
2. L.B. Hunt, *Platinum Metals Rev*, 4 (1969) 126
3. Z. B. Bao, H. Murakami, and Y. Yamabe-Mitarai, *Corros. Sci.*, 53 (2011) 1224
4. S. S. Serrano López, V. E. Reyes-Cruz, H. Rios-Reyes., and M.A. Veloz Rodríguez, *Adv. Mat. Res.*, 976 (2014) 179
5. C. S. Maayan, E. Noam, G. Eliezer, *Electrochim. Acta*, 88 (2013) 240
6. C. Dorfling, G. Akdogan, S.M. Bradshaw, J.J. Eksteen, *Hydrometallurgy*, 138 (2013) 21–32
7. Alguacil, F.J., Rev. Metal. *Madrid*, 31(1995) 246-255
8. P.P. Sun and M.S. Lee, *Hydrometallurgy*, 105 (2011) 334
9. T. M. Grajales, M. F. Palacios, and G. J. E. López, *El hombre y la máquina*, 28 (2007) 46
10. N. Schubert, M. Schneider and A. Michealis, *Electrochim. Acta*, 113 (2013) 748
11. K. Jüttner, U. Galla, and H. Schmieder, *Electrochim. Acta*, 45 (2000) 2575
12. G. Benke and W. Gnot, *Hydrometallurgy*, 64 (2002) 205

13. Saeid Kakooei, Mokhtar Che Ismail, Bambang Ari Wahjoedi, *J. Electrochem. Sci.*, 8 (2013) 3290-3301
14. S. Patrick and A. Elisabet, *Electrochim. Acta*, 68 (2012) 206
15. M. Jayakumar, K.A. Venkatesan, T.G. Srinivasan, P.R. Vasudeva-Rao, *Electrochim. Acta*, 54 (2009) 1083
16. P.S. Patil, R.K. Kawar and S.B. Sadale, *Electrochim. Acta*, 50 (2005) 2527
17. I. G. Casella, M. Contursi and T. Rosanna, *J. Electroanal. Chem.*, 736 (2015) 147
18. S. Le Vot, Lionel Roué, Daniel Bélanger, *Electrochim. Acta*, 59 (2012) 49–56
19. S.S. Serrano-López, V.E. Reyes-Cruz, M.A. Veloz-Rodríguez, J.M. Domínguez, *International Mexican Congress on Chemical Reaction Engineering (IMCCRE 2014)*, Acapulco, México, (2014) 210
20. M. Alon, A. Blum, E. Peled, *J. Power Sources*, 240 (2013) 417e420
21. F. Hisaaki, A. Tetsuya, Y. Masaaki, I. Tatsuo and K. Roland, *ISIJ Int.*, 33 (1993) 9 I009-1015
22. N. Garcia-Araez, V. C., Paramaconi Rodriguez and J. M. Feliu, *Langmuir* 26 (2010) 12408–12417
23. M. Goor-Dar, N. Travitsky, E. Peled, *J. Power Source*, 197 (2012) 111–115
24. J. Eugene. Kelly and H. R. Bronstein, *J. Electrochem. Soc.* 131 (1984) (10): 2232-2238
25. I. T.E. Fonseca, M. Irene Lopes, M. Teresa C. Portela, *J. Electroanal. Chem.*, 415 (1996) 89-96
26. A. V. Ermakov, S. M. Klotsman, S. A. Matveev, G. N. Tatarinova, A. N. Timofeev, V. K. Rudenko, N. I. Timofeev, and G. F. Kuzmenko, *Phys. Met. Metallog.*, *Metallogr*, 93 (2002) 435